Flame Height from Rectangular Fire Sources Considering Mixing Factor

OSAMI SUGAWA
Center for Fire Science and Technology
Science University of Tokyo
2641 Yamasaki, Noda, Chiba 278, Japan

HIROOMI SATOH
Kajima Institute of Construction Technology
2-19-1 Tobitakyu, Choufu, Tokyo 182, Japan

YASUSHI OKA
Center for Fire Science and Technology
Science University of Tokyo
2641 Yamasaki, Noda, Chiba 278, Japan

ABSTRACT

Measurements of visible flame heights were carried out under quiescent atmospheric condition using single and multiple rectangular fire sources, with and without walls and/or a floor, to correlate flame height with the heat release rate considering entrainment effect. Flame height, L_f, is formulated as a function of heat release rate, Q, and mixing factor, k_m, as $L_f \propto k_m^{2/(2n+3)} \cdot Q^{2/(2n+3)}$. The same configurations of multi fire sources but with and without walls and/or a floor produced different slopes in dimensionless correlation of the flame height, L_f/D, with $Q^{*\,2/(2n+3)}_{rec}$ due to entrainment effects. For both terms, we confirmed n=0 for single and unconfined line fire source(s), and n=1 for square or circular fire source(s).

Key words: line fire sources, flame merging, mixing factor, dimensionless heat release rate,

1. INTRODUCTION

Dimensional analysis of the diffusion flame geometry from a square or a circular single fire source has established the dependence of flame height on Q^2/D^5 [1] or on Q^*.[2] Flame geometry from a single fire source [3-5] and extension behavior [6,7] from a set of openings has been also studied. However, no clear and sufficient data exists to establish the flame geometry from multi line fire sources considering the source configurations and heat release rates change. If a fire occurs in some story of a tall building and produce extended flames from openings, a series of openings could be tread as line fire source. The extended flames from openings might merge together and cause serious damage to upper stories as were shown in the fire accident occurred in the First Interstate Bank [8]. This fire suggested the necessity of a study on flame merging and extension behavior with a wall. Tests were conducted to obtain the flame heights when flames extended along walls and merged changing the configrations of the line fire sources. The geometry of flames merged from two rectangular diffusion burners in parallel was also considered, changing the distance between the sources and the heat release rates. In this paper we describe the characteristics of flame geometry obtained experimentally from multiple fire sources as a func-

tion of the dimensionless heat release rate, Q^*_{rec}. We also consider the mixing factor for flame(s), which controls flame height due to the effects of entrainment.

2. THEORETICAL PROCEDURE

Let us assume that the flame is controlled by buoyancy, the flame is quasi-steady, and solid boundary effects at the walls are unimportant to the Reynolds number but are highly effective in blocking entrainment. Flame is treated as a fully developed, turbulent, and diffusion flame. The characteristic terms governing the mass flux in a flame can be estimated by D and W as the respective short and long periphery lengths of the burner and flame height L_f. Moreover, if we assume that all of the fuel reacts with stoichiometric air with an apparent mixing factor, k_m, up to the flame tip producing heat release of Q, the fuel supply is small compared to the air entrained, and upward velocity, u, can be expressed by a function of $u/V \propto (z/D)^n$:

$$m \cdot r \cdot k_m \propto \rho u \cdot dA \propto \rho_o \cdot V \cdot (z/l)^n \cdot W \cdot L_f \qquad (1)$$

where m is the fuel supply rate, r the stoichiometric air-to-fuel ratio, Taking H as the heat of combustion of the fuel, and V as the characteristic upward velocity, and invoking Froude modeling, V is substituted for by $(g \cdot L_f)^{1/2}$. Noting that $Q = m \cdot r \cdot H \cdot k_m$, equation (1) can be transformed to

$$Q/(r \cdot H \cdot k_m) \propto \rho_o \cdot g^{1/2} \cdot L_f^{(2n+3)/2} \cdot W \cdot (1/D^n). \qquad (2)$$

Thus the dimensionless flame geometry L_f/D is estimated as a function of heat release rate and burner geometry:

$$(L_f/D) \propto [(Cp \cdot T_o)/(r \cdot H \cdot k_m)]^{2/(2n+3)} \cdot [(Q/\rho_o \cdot Cp \cdot T_o \cdot g^{1/2} \cdot W \cdot D^{3/2})]^{2/(2n+3)} \qquad (3)$$

which identifies the dimensionless groups of flame geometry and heat release rate. The second term of equation (4) is expressed in a dimensionless form following Zukoski et al.[3]:

$$Q^*_{rec} = Q/\rho_o \cdot Cp \cdot T_o \cdot g^{1/2} \cdot W \cdot D^{3/2} \qquad (4)$$

In the flame region, it was reported that upward velocity changes along the height from the fire source and is expressed by the following equations according to the geometry of the fire source,

$$u/V \propto (z/D)^n, \quad n=0 \text{ for line a fire source [4]} \qquad (5a)$$

and

$$u/V \propto (z/D)^n, \quad n=1/2 \text{ for a square or circular fire source [5]} \qquad (5b)$$

Substituting equation (5) into (4) and assuming $(Cp \cdot T_o/r \cdot H)$ is almost constant since it depends on fuel material and flame temperature, we can write the flame height as the dimensionless correlation of

$$(L_f/D) \propto k_m^{2/(2n+3)} \cdot Q^{*\,2/(2n+3)}_{rec}. \qquad (6a)$$

or

$$L_f \propto k_m^{2/(2n+3)} \cdot Q^{2/(2n+3)}. \qquad (6b)$$

The mixing factor, k_m, might be a function of fire source configuration

and of apparent flame surface area to ambient air. It should be noted that the dependence of the upward velocity along the characteristic vertical axis, L_f/D, is significant essentially only in the flame region.

3. INSTRUMENTATION and PROCEDURE

3-1. Fire Scenario and Building Model

A fire scenario of fully developed fire was taken in this test which occurred in a 40 m x 60 m plan pf tall building (as the standard floor with 75% rentable ratio) with a 30 kg/m^2 fire load (designed for its office section). The maximum heat release rate from openings for 30 min fire duration was estimated as 314 MW. Rectangular solid type reduced scale models of 1/50 and of 1/100 were made from stacked calcium silicate boards. The models were surrounded by wire mesh to prevent the wind effect and were located under a smoke collector during the tests.

3-2. Gas Diffusion Burner

The gas diffusion burner contained fine sand as a diffuser in a rectangular stainless steel vessel. In order to obtain the basic flame behavior from single line fire source in the first experiment, we used rectangular burners with various aspect ratios of 1:6, 1:8.8, 1:12, 1:17.8, 1:40, and 1:60. The second and third experiments were carried out mainly using rectangular gas diffusion burners in two sets of 2 cm x 120 cm and 2 cm x 60 cm for the 1/50 scale model, and another two sets of 1 cm x 40 cm, and 1 cm x 60 cm for the 1/100 model. These burners were composed in the configuration square, U or C-shaped, L-shaped, and parallel. Propane gas was used as a fuel and was supplied through controllable gas flow meters. We evaluated the heat release rate for the scale models according to the maximum heat release rate of 314MW keeping similarity of the flame length based on dimensionless heat release rate. [9]

3-3. Visual Recordings of Flame Height

Measurements were made mainly on visible flame heights, changing the gas flow rates and the congigurations of the burners. Four measurements methods were carried out, i.e. (1) infrared-imaged pictures, (2) judgments by eyes, (3) usual photographs, and (4) video tape recordings (video camera: JVC GX-S700). After the flame showed a quasi-steady state, 3 minutes after ignition in most cases, flame tip locations in 300 successive frames of video recordings were estimated directly on a CRT [9] and adopted as a flame height, L_f, from the burner surface. The flame tip location in each picture and each video frame was taken as the visible flame height.

4. RESULTS and DISCUSSION

4-1. Comparison of flame heights obtained by different methods

The flame heights depend strongly on the definition as well as the observation or recording methods. A temperature contour was set at 250°C in the IR image picture, and the highest position of the contour line was defined as the flame tip. A comparison between the average flame heights obtained from video recordings, eye-averaged, and IR image-picture are shown in Figure 1. The agreement between these is good although there is some scattering, which is essentially due to fluctuations of the flames. Thus, for the sake of estimating without personal difference in eye-averaged and presenting the quantitative flame heights, we adopted mainly the data from the video tape recordings.

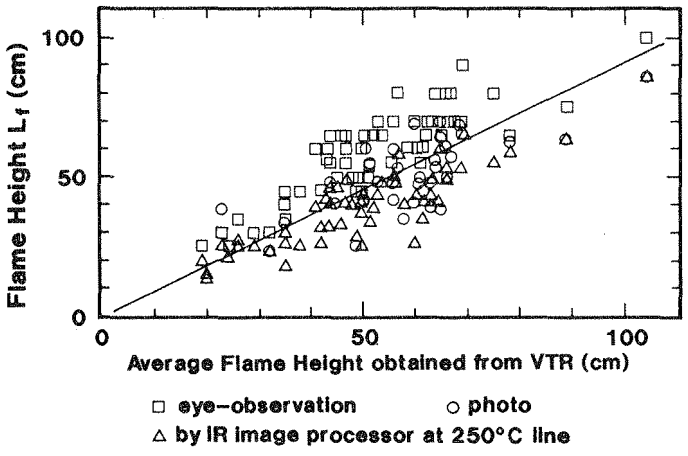

Figure 1 Comparison between flame heights obtained from video tape recording (averaged from 300 successive frames of pictures) and those obtained by eye averaged by color photos and by IR image processor.

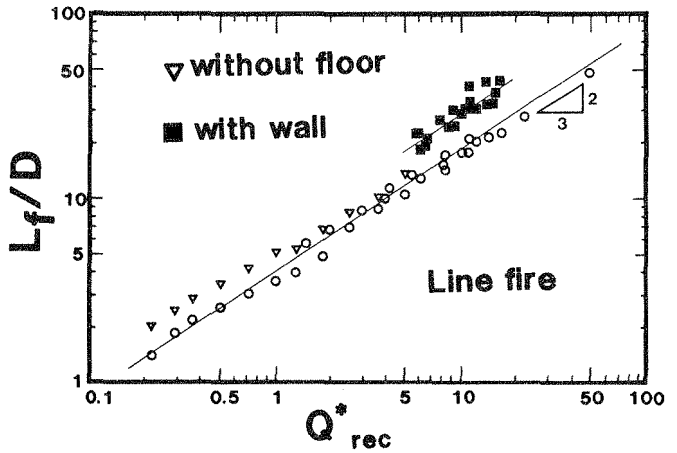

Figure 2 Dependence of flame height in dimensionless form on heat release rate in dimensionless form. Data were obtained from a line fire source using an unconfined rectangular propane gas diffusion burner without wall (○ , ▽) and against wall (■).

4-2. Flame Geometry from Single Rectangular (Line) Fire Source

In advance of the experiments setting the burners in the building model, similar tests without using the building model were made not only for the reference but for the basic flame behavior investigation. A rectangular burner was set about 50 cm above the floor. Figure 2 summarizes the dimensionless visible flame height, L_f/D, as a function of dimensionless heat release rate, Q^*_{rec}, based on the various aspects of the rectangular burners. The flame height, which is controlled in large part by the completion of combustion reaction, is approximately proportional to $Q^{*\,2/5}_{rec}$, and this implies that flame height should be

practically a function of heat release rate and independent of the amount of fuel and the aspect ratio in regard to our tests. For the range of $0.2 < Q^*_{rec} < 50$, the flame height is practically expressed by:

$$L_f/D = 4.2 \cdot Q^{*\,2/3}_{rec} \quad \text{(flame tip)} \tag{7}$$

The coefficient in the above equation, 4.2, is almost identical to the one reported by Delichatsios [10], and is an intermediate value compared with these of Hasemi [11]. Some data were obtained with a floor, and are plotted in Figure 2, showing the similar functional correlation by equation (7). However, the flame heights obtained in the presence of a floor are approximately 20 percent higher than surface of the floor. In the range of $0.2 < Q^*_{rec} < 50$, two distinct regions was not observed in the correlation between L_f/D and Q^*_{rec} for the flame from a line fire source as observed by Zukoski [12] for the flame from a circular burner.

4-3. Flame Geometry from narrow Multi-Rectangular (line) Fire Sources

a) Square configuration

Four line burners were set in a square configuration, and tests were carried out with and without a panel inside of the square. Figure 3 shows the dimensionless flame height, L_f/D, as a function of Q^*_{rec}. The plots of L_f/D without floor, triangles in Figure 3, lie closer to those from single rectangular burner as shown in Figure 2. However, when the void was covered with a panel, flames leaned toward the center forming higher flames compared with those with a void. The same flame extension behavior was observed when burners were located 30 cm (corresponding to 4 stories in the 1/50 scale model) down from the top of scale model. Thus, it is apparent that the flame geometry depends strongly on entrainment but little on the configuration.

b) C- and U-shaped configuration

Figure 4 shows the L_f/D as a function of Q^*_{rec}, with and without a floor. As a floor was not set, the height of the flame tips coincides generally with those in the unconfined single rectangular case, and is practically expressed also by equation (8). The flame heights obtained with floor and walls in the scale model are higher than those obtained without a floor when the same heat flux was given. The flame height is approximately proportional to $Q^{*\,2/5}_{rec}$. The effect on flame height by this configuration displayed the same behavior given by square configuration as described in the previous section.

c) L-shaped configuration

L_f/D obtained from L-shaped configlation were plotted against Q^*_{rec} in Figure 5. The lower slope of $L_f/D - Q^{*\,2/3}_{rec}$ was obtained when two rectangular fire sources located at the peripheries of the roof in scale model, and is also expressed by equation (8). When the model fire sources were located about 30 cm down from the top (simulating flames extended from openings of 4 stories down from the top) the highest flame heights was observed frequently at the corner due to flame merging as well as the decrease of entrainment due to the walls. Flame heights were higher than those located at the roof, and L_f/D are also plotted in Figure 5 showing the upper slope which is proportional to $Q^{*\,2/5}_{rec}$ in spite of the same heat release rates were used. In this configuration also, the same flame extension behavior due to the wall effect as described in the previous section was observed and was definitely confirmed.

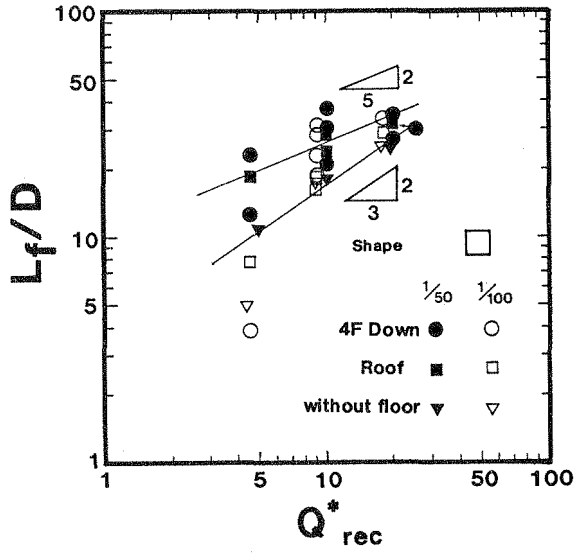

Figure 3 Dependence of flame height in dimensionless form on heat release rate in dimensionless form. Fire sources were arranged in a square configuration using four rectangular propane gas diffusion burners with models (●, ○, ■, □) and without models (▼, ▽).

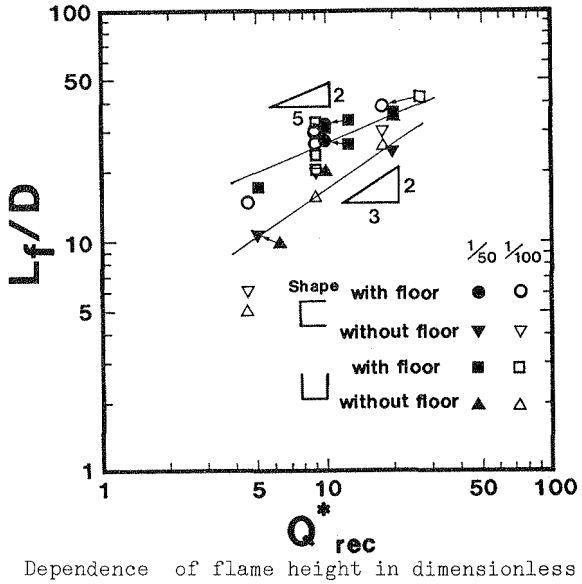

Figure 4 Dependence of flame height in dimensionless form on heat release rate in dimensionless form. Fire sources were arranged in a C shaped or U shaped configurations using three rectangular propane gas diffusion burners with models (●, ○, ■, □) and without models (▲, △).

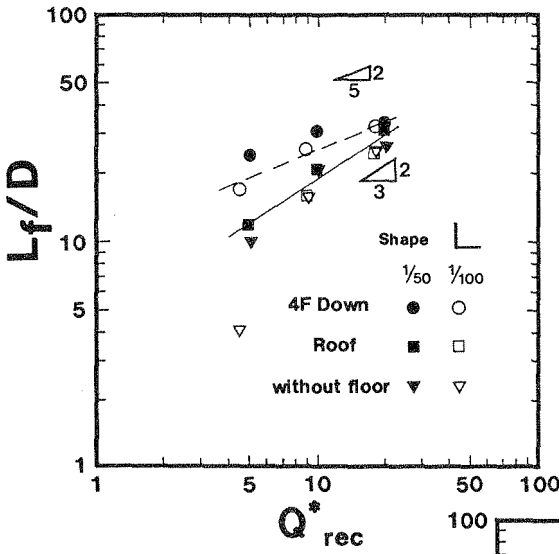

Figure 5 Dependence of flame height in dimensionless form on heat release rate in dimensionless form. Fire sources were arranged in a L shaped configuration using two rectangular propane gas diffusion burners with models (● , ○ , ■ , □) and without models (▼, ▽).

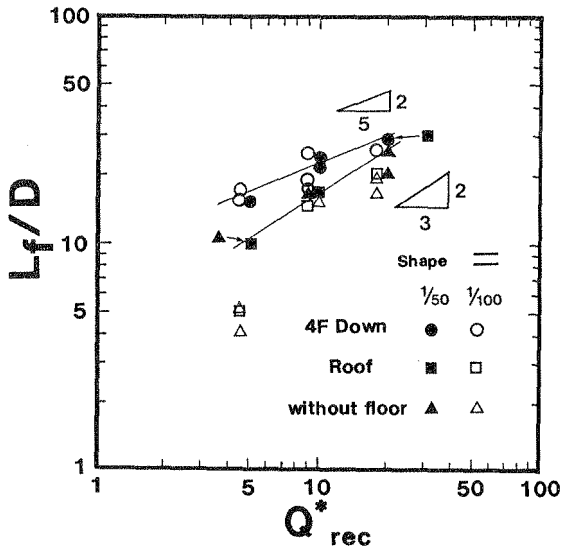

Figure 6 Dependence of flame height in dimensionless form on heat release rate in dimensionless form. Fire sources were arranged in a parallel configuration using two rectangular propane gas diffusion burners with models (● , ○ , ■ , □) and without models (▲, △).

d) Parallel line configuration

Two line fire sources in parallel were tested with and without a floor between them. The distance between sources, S, was set up to 40 or 80 times greater than length D, following the short and long sides of the plan of the rectangular scale models. The flame heights without floor and those from the sources set at the roof showed the same correlation as was expressed by equation (8). When the fire sources located 30 cm below the roof, the flame heights were higher than those without walls and are expressed as proportional to $Q^{*\,2/5}_{rec}$ as in Figure 6. The extension behavior of the flame due to prevention of entrainment by walls was the same as that confirmed in the previous section.

If the distance S decrease keeping the input heat release rate constant for two burners, flames from these sources begin to lean in and finally merge together, producing a higher flame than that from single fire source. Figure 7 shows the normalized flame height, L_f/L_{stand}, as

a function of the separation parameter, S/D. We adopt L_{stand} as a standard flame height which obtained for a single flame composed from two fire sources without separation at varying heat release rates of 1.25 l/min x 2 to 20 l/min x 2. In the separation parameter range of $0 < S/D < 4$, merged flame height looks 10 - 20 % higher than that of a standard flame, although it is in fluctuation. As the separation distance increases, the effect of merging on the flame extension decreases as shown in Figure 7, and the curve indicates a gradual approach to $L_f/L_{stand} = 0.63$. However, the tendency of flame extension due to merging was observed until the separation parameter exceeded 20.

5. Comparison of Experimental and Calculated Results on Flame Height

For a general presentation of flame height as a function of heat release rate and mixing factor due to boundaries effects, we tentatively assume that the mixing factor, $k_m^{2/(2n+3)}$ in equation (6b), is a function of flame geometry.

Entrainment blocked by a flame

As shown in Figure 7, the increase of separation produced an increase of apparent flame surface area to twice that in a no-separation case, with the total heat release rate constant. According to equation (6b), it can be held that 2-surfaces / 2-volumes of flames, which corresponds to the merged condition of 4-surfaces / 2-volumes of flames. This means that $k_m)_{mer}/k_m)_{iso} = 1/2$ with $Q)_{mer}/Q)_{iso} = 1$, which give the decrease of flame height as a factor of $1/2^{2/3}$ or 0.63. This estimated value agrees with the experimental data shown in Figure 7.

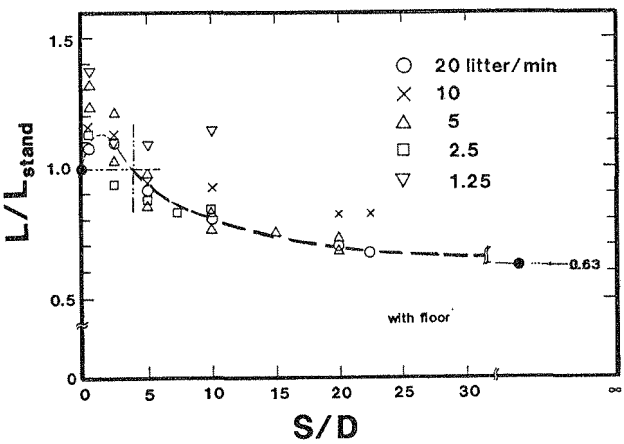

Figure 7 Dependence of flame height in dimensionless form on separation parameter S/D in dimensionless form. Fire sources were arranged in a parallel configuration using two rectangular propane gas diffusion burners. Gas flow rates varied from 1 25 l/min to 20 l/min per burner.

Entrainment blocked by a wall

Comparing the flame height from a line fire with wall(s) at a given heat release rate with those without wall(s), we can expect the mixing factor $k_m)_{free} / k_m)_{wall}$ to be 2, since half of the flame surfaces were covered by wall(s). Thus, the increase factor for the flame by $2^{2/3}$. In order to confirm the validity of our mixing factor model to the wall fire condition, calculations on the flame height with a wall have been performed based on the flame height from a single fire source plotted by in Figure 2. This correlation is described practically as,

$$L_f/D = 6.3 \cdot Q^*_{rec}{}^{2/3}. \qquad (8)$$

It is significant that the coefficient 6.3 in equation (8), which is almost equal to the $4.2 \times 2^{2/3}$ and is similar to the presentation for the flame tip height of the wall fire [11].

When the extended flame along a wall was partly or wholly covered with wall(s), for example $Q^*_{rec} = 5$ in Figure 3 - 6, flame height was about 24 cm with D = 2 cm, and the entire flame was covered with the wall of 30 cm long in the 1/50 scale model. Thus, the extended flame height in dimensionless form is expected to be $[24 \times (2)^{2/3}]/2 = 19$, which is very close to our measured value of 20 as shown in Figure 3 - 6. In the case of higher Q^*_{rec}, for example of 20, the flame height from a single burner of D = 2cm is about 60 cm, so that 30 cm of it is covered with wall and the remaining 30 cm extends beyond the wall. Thus the total dimensionless flame height for the 1/50 scale model is estimated as $[30 \times (2)^{2/3} + 30]/2 = 39$. This estimation is also very close to the measured value of 40, as shown in Figure 3 - 6.

Entrainment blocked by flames

We apply the same idea, expressed in equation (6b), to a flame merged from four pool fires that Koseki and Yumoto [13] have reported. They made a flame merged from four circular heptane pool fires in a dike, and obtained about 3m flame height from a pool fire source of 0.6m diameter, and merged flame height of about 5m from four pools, with a regression rate enhancement of 1.89 for each fire source. Hence, if we treat the merged fire as having 4 x 1.89 times greater heat release rate than a single source, the flame height increased by a factor of $(4 \times 1.89)^{2/5}$ was estimated. However, half of each plume merged was blocked by other plumes, so that half of the mixing $k_m)_{free}/k_m)_{mer} = 1/2$ is expected in this case. The actual entrainment will be $1/2^{2/5} \cdot (4 \times 1.89)^{2/5}$ which is about 1.70. Then, the merged flame height can be estimated as about 3 m x 1.7 = 5.1 m and which is very close to the height they reported.

6. SUMMARY and CONCLUSION

We found the power correlation between dimensionless flame height and dimensionles heat release rate with an entrainment mixing factor in the form of $L_f/D = k_m^{2/(2n+3)} \cdot Q^{*\,2/(2n+3)}_{rec}$ with k_m=8.6 and n=0 for a line fire, and k_m=28 and n=1 for square/circular fire source. This simple model is applicable to estimate the heights of flame extended not only by merging but also by blocking with wall(s) and flame(s).

7. ACKNOWLEDGMENT

The main experiments on the flame height observation were carried out in a facility of the Kajima Institute. Authors are grateful to staffs of the Kajima Institute and to Mr. Wataru Takahashi of the Center for Fire Science and Technology, for their assistance in carrying out the experiments.

8. REFERENCES

1) Thomas, P.H.,Webster, C.T., and Raftery, M.M."Some Experiments on Buoyant Diffusion Flames", Comb. and Flames vol.5, pp.359-367, (1961)
2) Zukoski,E.E., Kubota, T., and Cetegen, B. "Entrainment in Fire Plumes", Fire Safety Journal, vol.3, pp.107-121, (1980/81)
3) Yokoi, S. "Upward Current from an Infinite Line Fire Source"

(written in Japanese), Bulletin of the Fire Prevention Society of Japan, vol.10, No.1 (1961)
4) McCaffrey, B.J. "Purely Buoyant Diffusion Flames: Some Experi mental Results", NBSIR 79-1919, Nat. Bur. of Stand., Oct. (1979)
5) Thomas, P.H."The Size of Flames from Natural Fire", Ninth Symposium (International) on Combustion, pp.844-859, (1963)
6) Heskestad,G."Virtual Origins of Fire Plumes", Fire Safety Journal vol.5, pp.109-114, (1983)
7) Nitta, K., and Terai,T."On the Plume Rising from Liquid Fuels" Annual meeting of Kinki Regional Branch, Architectural Institute of Japan, pp.65-68 (1976)
8) Nelson, E.H.,"An Engineering View of the Fire at the First Inter State Bank Building", Fire Journal, pp.29-34, July/August (1989)
9) Sugawa, O.,Kawagoe,K.,Oka,Y., and Takahashi, K.,"Experimental Study on Extended Flame Behavior from an Opening using a Full Scale and a Reduced Scale Model", AIAA/ASME Thermophysics and Heat Transfer Conference, HTD vol. 141, pp.71-76, ASME (1990)
10) Delichatsios, M.A. "Flame Heights in Buoyant Diffusion Flame" Factory Mutual Research Corporation, FMRC Memo, March (1983)
11) Hasemi, Y. "Experimental Wall Flame Heat Transfer Correlations for the Analysis of Upward Wall Flame Spread", Fire Science and Technology, vol.4,No.2, pp75-90, (1984)
12) Cetegen,B.M., Zukoski,E.E., and Kubota, T.,"Entrainment and Flame Geometry of Fire Plumes", Cal. Inst. of Tech., August, (1982)
13) Koseki, H., and Yumoto T., "Burning Characteristics of Heptane in 2.7m Square Dike Fires", Proceeding of the Second International Symposium, pp.231-240, June, (1988)

9. NOMENCLATURE

A: horizontal area of plume
Cp: specific heat of air
D: characteristic short length of a rectangular fire source or characteristic size of fire source
H: heat of combustion
L_f: averaged flame height defined as a position of flame tip
Q: heat release rate
Q^*_{rec}: dimensionless heat release rate defined as

$$Q^*_{rec} = Q / \cdot Cp \cdot T_o \cdot g^{1/2} \cdot D^{3/2} \cdot W$$

g: acceleration of gravity
k_m: mixing factor depend on the fluid dynamics effected by wall(s) or flame(s)
r: stoichiometric oxygen to fuel mass ratio
S: surface area
u: upward flame velocity
V: characteristic flame velocity
Vol: volume
W: characteristic long length of a rectangular fire source
z: vertical coordinate
ρ: density

Suffix

o: ambient f: flame rec: rectangular
mer: merged flame iso: isolated flame